

Improvement for Testing the Gravitational Inverse-Square Law at the Submillimeter Range

Wen-Hai Tan¹, An-Bin Du¹, Wen-Can Dong¹, Shan-Qing Yang^{1,2,*}, Cheng-Gang Shao¹, Sheng-Guo Guan^{1,3},
Qing-Lan Wang⁴, Bi-Fu Zhan⁵, Peng-Shun Luo¹, Liang-Cheng Tu^{1,2} and Jun Luo^{1,2,†}

¹MOE Key Laboratory of Fundamental Physical Quantities Measurement & Hubei Key Laboratory of Gravitation and Quantum Physics, PGMF and School of Physics, Huazhong University of Science and Technology, Wuhan 430074, People's Republic of China

²TianQin Research Center for Gravitational Physics and School of Physics and Astronomy, Sun Yat-sen University (Zhuhai Campus), Zhuhai 519082, People's Republic of China

³College of Physics and Communication Electronics, Jiangxi Normal University, Nanchang 330022, People's Republic of China

⁴School of Science, Hubei University of Automotive Technology, Shiyan 442002, China

⁵School of Electrical and Electronic Engineering, Wuhan Polytechnic University, Wuhan 430023, People's Republic of China

(Received 19 November 2019; revised manuscript received 5 January 2020; accepted 21 January 2020; published 5 February 2020)

We improve the test of the gravitational inverse-square law at the submillimeter range by suppressing the vibration of the electrostatic shielding membrane to reduce the disturbance coupled from the residual surface potential. The result shows that, at a 95% confidence level, the gravitational inverse-square law holds ($|\alpha| \leq 1$) down to a length scale $\lambda = 48 \mu\text{m}$. This work establishes the strongest bound on the magnitude α of the Yukawa violation in the range of 40–350 μm , and improves the previous bounds by up to a factor of 3 at the length scale $\lambda \approx 70 \mu\text{m}$. Furthermore, the constraints on the power-law potentials are improved by about a factor of 2 for $k = 4$ and 5.

DOI: 10.1103/PhysRevLett.124.051301

Gravity is well described by the general relativity, which is verified by all the experiments and observations to date, and consistent with the Newtonian inverse-square law (ISL) in the nonrelativistic limit in a weak gravitational field. However, the general relativity has not been quantized successfully, and the gravity is poorly characterized in the short range. For unifying the gravity and the other three fundamental interactions, a number of speculations have been proposed and predict a deviation from the gravitational inverse-square law in a short-range regime [1–8], as well as some new light bosons predicted by the extension to the standard model [9]. The deviations from the ISL are usually parametrized by a Yukawa potential

$$V(r) = -G \frac{m_1 m_2}{r} (1 + \alpha e^{-r/\lambda}), \quad (1)$$

where G is the Newtonian gravitational constant, α is the strength of any new interaction, which is assumed to be a universal constant and insensitive to the compositions, λ is the length scale, and r is the separation between two masses. For searching the new interactions, a large number of experiments have been performed [10–27]. The detailed and comprehensive reviews about the predictions and experiments are available in Refs. [28–32]. Setting stringent limits on α for small λ requires small separations, $r \lesssim \lambda$, in order for test bodies to interact significantly.

In this Letter, we report a new constraint on the Yukawa type violation. The setup was based on our previous experiment, that tested the ISL using a torsion balance with dual modulation and compensation at the separation of 295 μm [24], as shown in Fig. 1, but the driving unit of the attractor was improved for reducing the electrostatic disturbance caused by the vibration of the shielding membrane between the pendulum and the attractor. With the improvement, the separation between the test and source masses was shortened down to 210 μm , in which the pendulum-membrane separation was 90 μm . The violation parameters were estimated by the maximum likelihood method with the data taken at several separations.

The schematic of the experiment is shown in Fig. 1. The attractor was eightfold azimuthal symmetric, and rotated about a horizontal axis which allowed the Yukawa force to be detected in the most sensitive direction of the torsion balance. The driving frequency was set to $\omega_d = 1.634 \text{ mrad/s}$, and the signal frequency was put at $8\omega_d$, to separate the disturbances at the fundamental frequency, and located at the low noise frequency band. The I-shaped pendulum with the $14.610 \times 0.200 \times 12.003 \text{ mm}^3$ tungsten test masses and $14.610 \times 0.289 \times 12.003 \text{ mm}^3$ gravitational compensation masses attached on the side of two ends, was suspended by a 70-cm-long, 25- μm -diameter tungsten fiber. The attractor consisted of eight $17.597 \times 0.200 \times 11.403 \text{ mm}^3$ tungsten

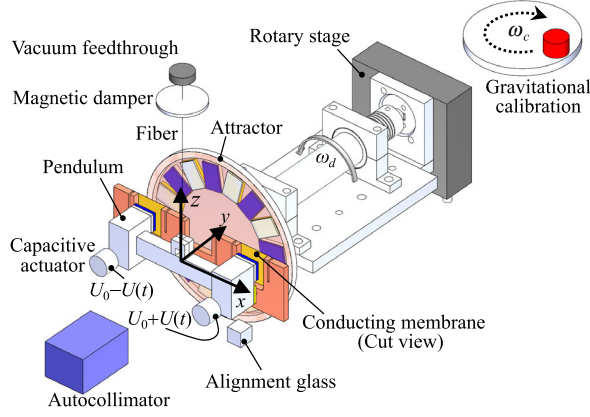


FIG. 1. Schematic drawing of the experimental setup (not to scale). Compared with our previous experiment [24], the rotary stage was replaced by a smaller and vacuum compatible one, and installed at the end of the rotary shaft. The attractor and the rotary stage, as well as the alignment glass, are supported on a 6-degree-of-freedom stage to adjust the position (not shown here). The electrostatic shielding membrane was placed on a translation stage to adjust the separation between the pendulum.

source masses and eight $17.597 \times 0.219 \times 11.403 \text{ mm}^3$ compensation masses, which arrayed alternatively on a 100-mm-diameter, 3-mm-thick glass disk. The relative position of the attractor and the alignment glass was measured by a coordinate measuring machine during the assembly, and the attractor was aligned with the pendulum by the 6-degree-of-freedom stage in vacuum. Using the dual compensation design, a null experiment was realized with the $8\omega_d$ Newtonian torque of $(0.4 \pm 0.5) \times 10^{-17} \text{ N m}$ at the separation of $210 \mu\text{m}$. The sensitivity of the closed-loop pendulum was calibrated by the gravitational signal from a rotating copper cylinder, which had a weight of 1140 g, the rotation frequency of $\omega_c = 15.7079 \text{ mrad/s}$, and located outside the vacuum chamber. More details about the setup can be found in Ref. [24].

In the short range, the electrostatic disturbance is dominant. Two 30- μm -thick electrostatic shielding membranes were inserted between two ends of the pendulum and the attractor. As the electrostatic disturbance made the pendulum unstable, a proportional-integral-differential (PID) electrostatic feedback control system was used to maintain the pendulum at the stable position. Considering the internal damping [33], the equation of motion of the closed-loop torsion pendulum is

$$I\ddot{\theta} + k(1 + i/Q)\theta - k_e\theta = \tau - \beta U, \quad (2)$$

where the moment of inertia of the pendulum $I = (6.977 \pm 0.002) \times 10^{-5} \text{ kg m}^2$, the spring constant $k = (8.05 \pm 0.06) \times 10^{-9} \text{ N m/rad}$, the quality factor $Q \approx 2500$. The feedback voltage U was calculated from the twist of the pendulum θ with PID algorithm. $\beta = (4.7 \pm 0.3) \times 10^{-13} \text{ N m/V}$ is the ratio of the control

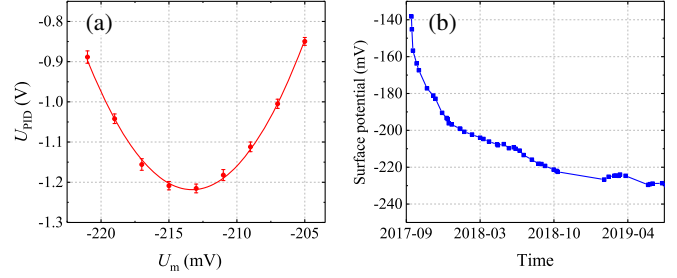


FIG. 2. (a) The feedback voltage U_{PID} of the closed-loop torsion balance is a minimum when the potential U_m applied on the shielding membrane equals to the surface potential difference between the pendulum and the membrane. The solid line is the parabolic fit to the experiment data. (b) The potential difference varies with time obviously after the chamber vacuumized, and the drift slows down as time increased. The results for the other membrane are similar.

torque to the feedback voltage U , which depends on the sizes, the separations, and the bias voltage of the control electrodes. τ is the torque exerted on the pendulum, including the Yukawa signal to be detected, the calibration signal, the residual Newtonian torque, the thermal noise, etc., $k_e = \partial\tau_e/\partial\theta$ was the negative spring constant of the electrostatic interaction between the pendulum and the shielding membrane, where $\tau_e = (-1/2)(\partial C/\partial\theta)\Delta U^2$ was the electrostatic torque between the pendulum and the shielding membrane, with the capacity C and the residual surface potential difference ΔU .

The surface potential differences between the pendulum and the membrane were due to the contact potential for different metals and the patch effect from the imperfect surfaces of the conductors. It was determined by applying a stair-changed voltage on each shielding membrane and found the extremum of the control voltage of the closed-loop torsion balance. The typical result for one membrane was shown in Fig. 2(a), and the surface potential for different data runs during about 2 years were shown in Fig. 2(b), which approximately decays exponentially. For reducing the electrostatic disturbances, the surface potential of each membrane was compensated to equipotential with the pendulum by a voltage source meter with accuracy of 0.6 mV for each data run.

To evaluate if there is potential variation on the shielding membrane that induced by the rotating attractor, we used a $7\frac{1}{2}$ -digit high performance multimeter to measure the voltage on the membrane, while the compensation voltage had been applied, and the attractor was rotating. No signals appeared at any harmonic of the driving frequency, and the noise floor is less than $10 \mu\text{V}/\sqrt{\text{Hz}}$ around several millihertz. The corresponding torque noise is $\delta\tau_{eu} = [\partial\tau_e/\partial(\Delta U)]\delta U$, where $[\partial\tau_e/\partial(\Delta U)] = (8.4 \pm 0.5) \times 10^{-12} \text{ N m/V}$ was determined by measuring the torques responded to the modulated voltages applied on a shielding membrane, with the pendulum-membrane separation of $90 \mu\text{m}$. The voltage

noise introduces a torque noise of 9×10^{-17} N m/ $\sqrt{\text{Hz}}$, which is far below the thermal noise 2×10^{-15} N m/ $\sqrt{\text{Hz}}$ of the torsion balance with $Q \approx 2500$. The four-day data show that δU at the $8\omega_d$ is less than 17 nV, which introduces a torque noise less than 2×10^{-19} N m, and can be ignored.

Considering the parallel-plate capacitor model, the residual electrostatic torque should be zero when the potential of the membrane was compensated to the minimum shown in Fig. 2(a). However, due to the spatial variations of the patch potentials on the pendulum and the shielding membrane, some residual electrostatic torque still exists [34–38], and increases in a shorter range. Furthermore, the spacial distribution of the surface potential is difficult to be determined. As a result, the variation of the separation would introduce the torque noise or systemic errors, and must be considered more carefully in shorter range.

For the tiny vibration $\delta\theta_m$ of the shielding membrane around the vertical direction, the variation of the electrostatic torque is $\delta\tau_{e\theta} = k_e\delta\theta_m$, where $k_e = (2.6 \pm 0.4) \times 10^{-8}$ N m/rad with the pendulum-membrane separation of $90 \mu\text{m}$ as in the most data runs of this work. k_e were deduced from the response of the feedback voltage to the known gravitational calibration signal for each data run, according to Eq. (2).

In our previous experiment, a rotary stage was employed to drive the attractor from outside the vacuum chamber to reduce the temperature and electromagnetic disturbances. However, due to the uncoaxiality between the rotary stage, the feedthrough of the vacuum chamber, and the attractor, the stability of the shielding membrane became worse while the rotary was working. For reducing this disturbance, the rotary was replaced by a smaller and vacuum compatible version, which is mounted through a flexible connector directly at the end of the rotation shaft that fixed to the attractor. The stability of the shielding membrane was improved by more than an order of magnitude, that the rotation $\delta\theta_m$ around the vertical direction was reduced from (1.8 ± 0.1) nrad to (0.1 ± 0.1) nrad. The disturbance of the torque from $\delta\theta_m$ was estimated as $< 0.4 \times 10^{-17}$ N m at the pendulum-membrane separation of $90 \mu\text{m}$. This improvement allowed us to shorten the separation between the test and the source masses down to $210 \mu\text{m}$, where the possible Yukawa torque with smaller λ was increased compared with our previous experiment with $295\text{-}\mu\text{m}$ separation.

To increase the accuracy of the experiment, we used a “null” experiment to test the Yukawa effect, in which the Newtonian torque at $8\omega_d$ is well compensated when the attractor is aligned with the pendulum. In another case, when the attractor is misaligned, the $8\omega_d$ Newtonian torque increases significantly, namely the “non-null” experiment, which can verify the instruments further. Non-null experiments were performed with the attractor move 250 and $500 \mu\text{m}$ along the x direction, while keeping the separation at $210 \mu\text{m}$ between the test and the source masses, and $90 \mu\text{m}$ between the test mass and the shielding membrane.

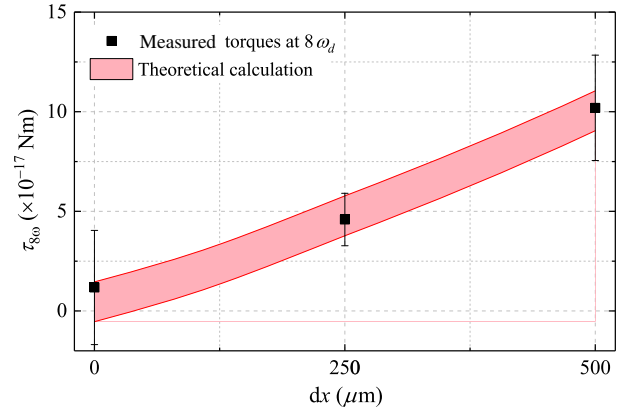


FIG. 3. “Non-null” experiment of the $8\omega_d$ component as the attractor’s position changed along the x direction, with the separation between the test and the source masses fixed to $210 \mu\text{m}$. The solid points are the measured values, and the shaded belt represents the theoretical calculations, both with the 2σ error.

The torque signal is deduced from the feedback voltage in the frequency domain. The voltage signal is $U(\omega_s) = (2/T) \int_0^T U(t) \exp(i\omega_s t) dt$ with $\omega_s = 8\omega_d$, and so does the calibration signal $U(\omega_c)$. The measured torque is $\tau(\omega_s) = [U(\omega_s)/U(\omega_c)][H_U(\omega_c)/H_U(\omega_s)]\tau_c(\omega_c)$, where $H_U(\omega) \equiv U(\omega)/\tau(\omega)$ is the transfer function according to Eq. (2), $\tau_c(\omega_c)$ is the calibration torque. Refer to Ref. [24] for more detail. The results of the non-null experiments are shown in Fig. 3, which shows the consistency of the measured torques and the theoretical Newtonian torques calculated from the geometric parameters.

Considering that the possible Yukawa signal should increase quickly as the separation between the test and source masses decreases, we tested the Newtonian inverse-square law at several separations for comparison, including 210, 230, 295, and $1095 \mu\text{m}$. The $8\omega_d$ torques are shown in Fig. 4, with the collected data length from about six to nine weeks. The tiny residual Newtonian torques are subtracted individually for each separation, which are not more than 1.5×10^{-17} N m for all the experiments above. All the results are consistent with zero at the 1σ level, indicating that no violation of the Newtonian inverse-square law was observed.

To make full use of the data at different separations for setting a stronger bound on the Yukawa effect, the maximum likelihood estimate method was used to determine the violation parameters [25], using the in-phase components of the residual torques at the four separations shown in Fig. 4. Considering the measured results are normal distributions, the likelihood function is defined as

$$P(\tau_m, \tau_i; \alpha, \lambda) = \prod_i \frac{1}{\sqrt{2\pi}\sigma_i} e^{-[(\tau_{mi} - \tau_{ii})^2 / 2\sigma_i^2]}, \quad (3)$$

where $i = 1, 2, 3, 4$, denotes the different test-source masses separations of $d_i = 210, 230, 295, 1095 \mu\text{m}$, τ_m

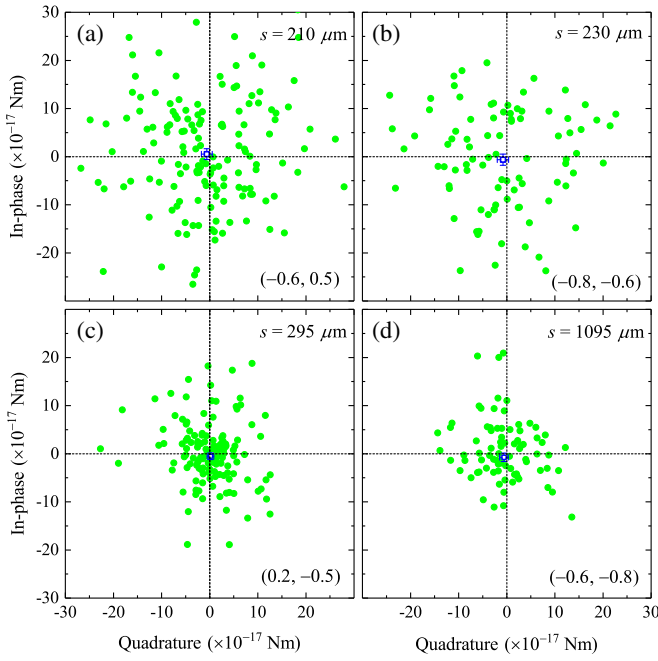


FIG. 4. The $8\omega_d$ measured torques at 210, 230, 295, and 1095- μm separations, respectively. Each solid dot represents a value obtained from a 10-rotation-period data segment, and the squares represent the mean values (shown in brackets) with the 1σ error of about 1×10^{-17} N m.

are the in-phase component of the measured torques, τ_i are the possible $8\omega_d$ Yukawa torques τ_Y that calculated from the violation parameters α , λ , and the geometric parameters. It is obtained by numerical integration $\tau_Y(d_i, \phi) = \int (\partial/\partial\theta)[(G\rho_j\rho_k/r)\alpha e^{-r/\lambda}]dV_jdV_k$ for different rotation angle ϕ of the attractor at the separation d_i , where V_j is the volume of the pendulum's components with density ρ_j , and the similar notation with subscript k denotes the parameter of the attractor's components. The total error $\sigma_i = \sqrt{\sigma_{mi}^2 + \sigma_{ti}^2}$, where σ_{mi} is the error of τ_{mi} , and σ_{ti} is the error of τ_{ti} that caused by the geometric parameters.

By searching α to maximize the likelihood function $P(\tau_m, \tau_i; \alpha, \lambda)$ for each value of λ , the best estimate α_e is determined, and the bound with 95% confidence level is found by $(1/A) \int_{\alpha_e - \delta\alpha}^{\alpha_e + \delta\alpha} P(\tau_m, \tau_i; \alpha, \lambda) d\alpha = 95\%$, where A is the normalization coefficient that ensures the total probability is 100% over all the α , and the constraint of $|\alpha|$ is set by the max one of $|\alpha_e - \delta\alpha|$ and $|\alpha_e + \delta\alpha|$, as shown in Fig. 5 with $\lambda = 100 \mu\text{m}$, for example. The constraints of $|\alpha|$ for other values of λ are calculated similarly, which are summarized in Fig. 6. It is the strongest bound on α in the range of 40–350 μm . At the length scale of $\lambda \approx 70 \mu\text{m}$, we improve the previous bounds by up to a factor of 3, and the inverse-square law holds ($|\alpha| \leq 1$) down to a length scale $\lambda = 48 \mu\text{m}$. For the two large extra-dimension scenarios with $\alpha = 16/3$ [29], the experiment requires the unification mass $M_* \geq 3.2 \text{ TeV}/c^2$ with the extra-dimension size $R_* \leq 37 \mu\text{m}$.

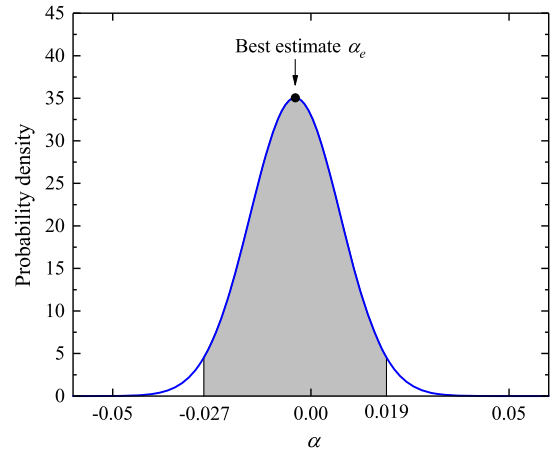


FIG. 5. Example of the probability density of α , considering $\lambda = 100 \mu\text{m}$. The shaded area represents the region of α with 95% probability. $\alpha_e = -0.004$ at the maximum is the best estimate of α . The constraint of $|\alpha| < 0.027$ is set by the max one of the absolute values of the lower limit ($\alpha_e - \delta\alpha$) = -0.027 and the upper limit ($\alpha_e + \delta\alpha$) = 0.019 . The constraints of $|\alpha|$ for other values of λ are calculated similarly.

The power-law potentials can arise from the higher-order exchange processes with a simultaneous exchange of multiple massless bosons [8], which is parametrized as

$$V_{ab}^k(r) = -G \frac{m_a m_b}{r} \beta_k \left(\frac{1 \text{ mm}}{r} \right)^{k-1}, \quad (4)$$

where β_k are the power-law parameters for $k = 2, 3, 4$ and 5. Using the similar analysis method as the Yukawa violation, we obtain the better constraints on β_k , which are listed in Table I.

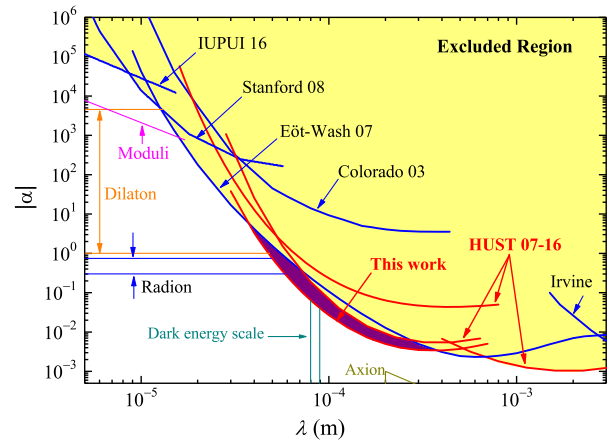


FIG. 6. Constraints on Yukawa violation of the Newtonian $1/r^2$ law. The shaded region is excluded at a 95% confidence level by this work, and the previous experiments from Refs. [10–14, 22–24], respectively. Light lines show various theoretical predictions summarized in Refs. [29,39].

TABLE I. Constraints on the power-law potentials with 68% confidence from this work and from previous result of Ref. [8].

k	$ \beta_k $ (this work)	$ \beta_k $ (Ref. [8])
2	3.7×10^{-4}	4.5×10^{-4}
3	7.5×10^{-5}	1.3×10^{-4}
4	2.2×10^{-5}	4.9×10^{-5}
5	6.7×10^{-6}	1.5×10^{-5}

The main uncertainty of the measured torque at the short range is the random noise, which increases quickly at the shorter range, indicating that the coupling of the vibration to the residual surface potential is still an important noise source. Improving the vibration isolation of the torsion pendulum and the shielding membrane should reduce this noise further.

This work was supported by the National Natural Science Foundation of China under Grants No. 11705061, No. 11722542, No. 91736312, and No. 91436212.

A.-B. D. and W.-H. T. contributed equally to this work.

*yshq@sysu.edu.cn

†junluo@sysu.edu.cn

- [1] N. Arkani-Hamed, S. Dimopoulos, and G. Dvali, *Phys. Lett. B* **429**, 263 (1998); *Phys. Rev. D* **59**, 086004 (1999).
- [2] S. Dimopoulos and G. F. Giudice, *Phys. Lett. B* **379**, 105 (1996).
- [3] S. R. Beane, *Gen. Relativ. Gravit.* **29**, 945 (1997).
- [4] R. Sundrum, *J. High Energy Phys.* **07** (1999) 001; *Phys. Rev. D* **69**, 044014 (2004).
- [5] D. B. Kaplan and M. B. Wise, *J. High Energy Phys.* **08** (2000) 037.
- [6] N. Arkani-Hamed, S. Dimopoulos, G. Dvali, and N. Kaloper, *Phys. Rev. Lett.* **84**, 586 (2000).
- [7] L. Randall and R. Sundrum, *Phys. Rev. Lett.* **83**, 4690 (1999).
- [8] E. G. Adelberger, B. R. Heckel, S. Hoedl, C. D. Hoyle, D. J. Kapner, and A. Upadhye, *Phys. Rev. Lett.* **98**, 131104 (2007).
- [9] J. E. Moody and F. Wilczek, *Phys. Rev. D* **30**, 130 (1984).
- [10] C. D. Hoyle, D. J. Kapner, B. R. Heckel, E. G. Adelberger, J. H. Gundlach, U. Schmidt, and H. E. Swanson, *Phys. Rev. D* **70**, 042004 (2004); D. J. Kapner, T. S. Cook, E. G. Adelberger, J. H. Gundlach, B. R. Heckel, C. D. Hoyle, and H. E. Swanson, *Phys. Rev. Lett.* **98**, 021101 (2007).
- [11] J. K. Hoskins, R. D. Newman, R. Spero, and J. Schultz, *Phys. Rev. D* **32**, 3084 (1985).
- [12] R. S. Decca, D. López, H. B. Chan, E. Fischbach, D. E. Krause, and C. R. Jamell, *Phys. Rev. Lett.* **94**, 240401 (2005); Y.-J. Chen, W. K. Tham, D. E. Krause, D. López, E. Fischbach, and R. S. Decca, *Phys. Rev. Lett.* **116**, 221102 (2016).
- [13] J. Chiaverini, S. J. Smullin, A. A. Geraci, D. M. Weld, and A. Kapitulnik, *Phys. Rev. Lett.* **90**, 151101 (2003); A. A. Geraci, S. J. Smullin, D. M. Weld, J. Chiaverini, and A. Kapitulnik, *Phys. Rev. D* **78**, 022002 (2008).
- [14] J. C. Long, H. W. Chan, A. B. Churnside, E. A. Gulbis, M. C. M. Varney, and J. C. Price, *Nature (London)* **421**, 922 (2003).
- [15] M. Masuda and M. Sasaki, *Phys. Rev. Lett.* **102**, 171101 (2009).
- [16] S. K. Lamoreaux, *Phys. Rev. Lett.* **78**, 5 (1997); A. O. Sushkov, W. J. Kim, D. A. R. Dalvit, and S. K. Lamoreaux, *Phys. Rev. Lett.* **107**, 171101 (2011).
- [17] M. Bordag, U. Mohideen, and V. M. Mostepanenko, *Phys. Rep.* **353**, 1 (2001); G. L. Klimchitskaya, U. Mohideen, and V. M. Mostepanenko, *Phys. Rev. D* **87**, 125031 (2013).
- [18] Y. Kamiya, K. Itagaki, M. Tani, G. N. Kim, and S. Komamiya, *Phys. Rev. Lett.* **114**, 161101 (2015).
- [19] M. V. Moody and H. J. Paik, *Phys. Rev. Lett.* **70**, 1195 (1993).
- [20] J. C. Long and V. A. Kostelecký, *Phys. Rev. D* **91**, 092003 (2015).
- [21] C.-G. Shao, Y.-J. Tan, W.-H. Tan, S.-Q. Yang, J. Luo, M. E. Tobar, Q. G. Bailey, J. C. Long, E. Weisman, R. Xu, and V. A. Kostelecký, *Phys. Rev. Lett.* **117**, 071102 (2016); C.-G. Shao, Y.-F. Chen, Y.-J. Tan, S.-Q. Yang, J. Luo, M. E. Tobar, J. C. Long, E. Weisman, and V. A. Kostelecký, *Phys. Rev. Lett.* **122**, 011102 (2019).
- [22] L.-C. Tu, S.-G. Guan, J. Luo, C.-G. Shao, and L.-X. Liu, *Phys. Rev. Lett.* **98**, 201101 (2007).
- [23] S.-Q. Yang, B.-F. Zhan, Q.-L. Wang, C.-G. Shao, L.-C. Tu, W.-H. Tan, and J. Luo, *Phys. Rev. Lett.* **108**, 081101 (2012).
- [24] W.-H. Tan, S.-Q. Yang, C.-G. Shao, J. Li, A.-B. Du, B.-F. Zhan, Q.-L. Wang, P.-S. Luo, L.-C. Tu, and J. Luo, *Phys. Rev. Lett.* **116**, 131101 (2016).
- [25] J. Wang, S. Guan, K. Chen, W. Wu, Z. Tian, P. Luo, A. Jin, S. Yang, C. Shao, and J. Luo, *Phys. Rev. D* **94**, 122005 (2016).
- [26] C. C. Haddock, N. Oi, K. Hirota, T. Ino, M. Kitaguchi, S. Matsumoto, K. Mishima, T. Shima, H. M. Shimizu, W. M. Snow, and T. Yoshioka, *Phys. Rev. D* **97**, 062002 (2018).
- [27] J. Liu and K.-D. Zhu, *Eur. Phys. J. C* **79**, 18 (2019).
- [28] E. Fischbach and C. L. Talmadge, *The Search for Non-Newtonian Gravity* (Springer, New York, 1999).
- [29] E. G. Adelberger, B. R. Heckel, and A. E. Nelson, *Annu. Rev. Nucl. Part. Sci.* **53**, 77 (2003); E. G. Adelberger, J. H. Gundlach, B. R. Heckel, S. Hoedl, and S. Schlamminger, *Prog. Part. Nucl. Phys.* **62**, 102 (2009).
- [30] R. D. Newman, E. C. Berg, and P. E. Boynton, *Space Sci. Rev.* **148**, 175 (2009).
- [31] J. Murata and S. Tanaka, *Classical Quantum Gravity* **32**, 033001 (2015).
- [32] M. S. Safronova, D. Budker, D. DeMille, D. F. J. Kimball, A. Derevianko, and C. W. Clark, *Rev. Mod. Phys.* **90**, 025008 (2018).
- [33] P. R. Saulson, *Phys. Rev. D* **42**, 2437 (1990).
- [34] C. C. Speake and C. Trenkel, *Phys. Rev. Lett.* **90**, 160403 (2003).
- [35] R. O. Behunin, D. A. R. Dalvit, R. S. Decca, and C. C. Speake, *Phys. Rev. D* **89**, 051301(R) (2014).

- [36] W.J. Kim, A.O. Sushkov, D.A.R. Dalvit, and S.K. Lamoreaux, *Phys. Rev. A* **81**, 022505 (2010).
- [37] F. Antonucci, A. Cavalleri, R. Dolesi, M. Hueller, D. Nicolodi, H.B. Tu, S. Vitale, and W.J. Weber, *Phys. Rev. Lett.* **108**, 181101 (2012).
- [38] H. Yin, Y.-Z. Bai, M. Hu, L. Liu, J. Luo, D.-Y. Tan, H.-C. Yeh, and Z.-B. Zhou, *Phys. Rev. D* **90**, 122001 (2014).
- [39] J.C. Long, H.W. Chan, and J.C. Price, *Nucl. Phys.* **B539**, 23 (1999).